International Journal of Engineering Trends and Technology
ISSN: 2231–5381 / https://doi.org/10.14445/22315381/IJETT-V71I5P239

Volume 71 Issue 5, 386-401, May 2023

Original Article

Combining Super Resolution and EfficientNet Models to Reduce False Positives and False Negatives in Breast Cancer Detection

Vandana Lingampally[1], Radhika Kavuri[2]

[1]*Department of CSE, Osmania University, Hyderabad, India*
[2]*Department of IT, CBIT, Hyderabad, India*

[1]*Corresponding Author : researchprojectphd9974@gmail.com*

Received: 22 January 2023 Revised: 17 April 2023 Accepted: 26 April 2023 Published: 25 May 2023

Abstract *- The accurate detection of breast cancer is imperative for optimal therapeutic outcomes, and minimizing false positive and false negative rates is a vital element in this process. Super-resolution images are particularly used in health research due to their ability to provide higher spatial resolution and more detailed information about the appearance of tissues and structures in medical images. These images can enable the model to learn to identify subtle abnormalities and distinguish them from normal tissue, and they are also more resistant to image degradation, such as noise or blur. To obtain high-resolution mammograms, a generator network (SRGAN) was trained and obtained SR images were applied on EfficientNet models, which are highly effective deep learning architectures that exhibit superior performance on a wide range of tasks with a reduced number of parameters and lower computational complexity compared to other models. A combination of three datasets (CBIS-DDSM, Mini-MIAS, and INbreast) with data augmentation was used to train and evaluate the model. The proposed model achieved a false positive and false negative rate of 0.0029, indicating a high level of accuracy in detecting breast cancer. This low rate highlights the efficacy of the approach in minimizing false positive and false negative rates, which is crucial for optimal treatment outcomes.*

Keywords *- Breast cancer, Deep learning, Efficientnet, SRGAN, Super-resolution.*

1. Introduction

False positives and false negatives in breast cancer detection can have significant consequences for patients. False positives, also known as false alarms, occur when a test incorrectly indicates the presence of cancer. This can lead to unnecessary additional testing, such as biopsies, which can be expensive and invasive for the patient. False positives can also cause anxiety and distress for the patient. On the other hand, false negatives, also known as missed diagnoses, occur when a test incorrectly indicates the absence of cancer. This can result in a delay in diagnosis and treatment, which can be particularly harmful in the case of breast cancer, as early detection is often key to successful treatment. False negatives can also lead to a false sense of security for the patient, causing them to forego necessary screenings in the future. It is, therefore, important to strive for high levels of accuracy in breast cancer detection methods in order to minimize both false positives (FP) and false negatives (FN).

1.1. Limitations of Current Breast Mass Classification Models

After analyzing several papers from previous research (presented in section 2), it can be observed that the percentage of FN and FP results in the classification of breast masses is high, with significant variation between the FN and FP percentages.

Despite the application of robust preprocessing techniques, advanced enhancement methods, and state-of-the-art deep learning models for feature extraction and classification, the classification accuracy of breast masses remains suboptimal. The primary question is why these models cannot accurately diagnose masses with high accuracy. Indeed, it appears that the limited information provided by low-resolution mammograms may be hindering the accuracy of breast mass classification. Therefore, more relevant features are necessary for accurate classification, which may ultimately lead to a reduction in the number of FP and FN results.

To overcome this limitation, high-resolution mammograms can be utilized to extract more detailed and comprehensive features that may be crucial for accurate classification. Incorporating this additional information into the models may enable them to make more accurate decisions, ultimately reducing the number of FP and FN.

1.2. High-Resolution Images

The image is a grid of individual pixels. Pixel density per inch gives the resolution of the image. Low resolution indicates less no. of pixels per inch, and high resolution indicates more pixels per inch. When no. of pixels is more per inch, the image will be of more clarity with much more details.

1.3. High-Resolution Mammograms

A mammogram contains information about the structure and tissue of the breast, which includes fatty tissue, ducts and lobules, and it also shows blood vessels in the breast. There may be the presence of abnormalities in the mammograms, like masses and calcifications, which will be small in size when compared with the full size of the breast. Detailed information on abnormalities is needed to decide whether the abnormalities are benign or malignant, which may not be seen in low-resolution mammograms and especially when the tissue is dense. So there is a need for high-resolution mammograms which give finer details or more detailed information about the abnormalities, which will help in deciding whether the abnormality is benign or malignant.

1.4. Methods to Acquire High-Resolution Mammograms

Interpolation methods: These methods use mathematical algorithms to estimate the values of missing pixels in an image, thereby increasing its resolution. Some frequently used methods for interpolation include the nearest neighbor, bilinear[1], and bicubic interpolation[2]. The bicubic interpolation method calculates the value of each new pixel by taking a weighted average of the 16 pixels that are closest in proximity, using a sophisticated algorithm to derive a precise approximation. This method may be effective at increasing the resolution of an image. Still, it introduces artifacts such as blurriness and ringing, which can reduce the image's level of detail and clarity.

1.4.1. CNNs

These deep learning models can be trained on pairs of LR and HR images, from which they can construct a mapping function to generate HR images from LR images. To construct mapping function 1. SRCNN[3] uses 3 convolutional layers, the initial layer acts as a feature extractor, the subsequent layer serves as a mapping layer, and the last layer acts as a reconstructor. 2. FSRCNN[4] uses feed-forward architecture and a deconvolutional layer. 3. ESPCN[5] uses sub-pixel convolutional layer. 4. VDSR[6] uses very deep network architecture with a residual learning strategy. 5. EDSR [7] uses deep residual network architecture with a high-capacity feature extractor. Many more CNN models have been introduced to generate high-resolution images, but the fact is that CNNs are introduced to recognize and classify images but not to generate images.

1.4.2. GANs

In these models, the generator network generates new images and is paired with a discriminator network that evaluates the generated images' authenticity. GANs can be used to synthesize HR images from LR ones by training the generator network to produce images that are similar to the original high-resolution ones. Many GAN models have been introduced to generate super-resolution images. Some of the models are SRGAN [8], ESRGAN [9], DCGAN [10], CGAN [11], and WGAN [12]. In this study, SRGAN was initially utilized to obtain the super-resolution mammograms, and other GAN models may be explored in future work.

1.5. Selection of Deep Learning Models

To optimize the performance of the deep learning model for breast cancer(BC) detection using super-resolution mammogram images, a series of experiments were conducted with various architectures. After evaluating the results, it was determined that the EfficientNet model demonstrated superior performance in terms of reducing both FN and FP. As a result, EfficientNet was selected as the most appropriate model for this task.

This paper provides a comprehensive review of relevant previous research in the field in Section 2. The dataset creation and proposed model are presented in detail in Section 3. The implementation procedure is explained, and the study results are analyzed for their significance in Section 4. Lastly, the findings are summarized, and potential avenues for future work are suggested in Section 5.

2. Related Work

Breast cancer has been a rising concern in both rural and urban parts of India, with an alarming estimated count of 224,000 new cases in the year 2021 alone. Over the past decade, the incidence rate of breast cancer in India has been increasing at a yearly pace of 5-6%. Unfortunately, the mortality rate for breast cancer in India remains relatively high, with an estimated 138,000 fatalities in the same year. Early detection is crucial as cancer survival becomes increasingly challenging in advanced stages, and it's disappointing to note that more than half of Indian women are detected with stages 3 and 4 of BC. The best way to curb the mortality rate is by detecting breast cancer in its initial stage to provide better chances of recovery.

Several recent studies have delved into breast cancer research to find ways to address the rising incidence and mortality rates in India. In this section, we present a selection of such literature that sheds light on the current state of breast cancer research.

It has been observed from Table 1. that the percentage of FP and FN is high, with significant variation between the FN and FP percentages. Despite the application of robust preprocessing techniques, advanced enhancement methods, and state-of-the-art deep learning models for feature extraction and classification, the classification accuracy of breast masses remains suboptimal.

Table 1. Presents details of a few research papers

Sl. No	Author	Methods/Models	Accuracy %	False Negative %	False Positive %
1	Pak F [22] (2015)	(Mini-MIAS), NSCT for feature extraction and Adaboost for classification	91.43	12.85	6.42
2	Al-Antari MA [27] (2018)	(Inbreast), YOLO for mass detection, FrCN for mass segmentation, CLAHE for enhancement, AlexNet with few changes for extraction and classification	90.00	2.00	30.00
3	Ragab B [26] (2019)	(CBIS-DDSM, DDSM), threshold and region-based methods for segmentation, CLAHE for enhancement, AlexNet for extraction and SVM for classification	87.20	13.80	12.30
4	Ridhi A [32] (2020)	(CBIS-DDSM), histogram equalization for enhancement, an ensemble of AlexNet, VGG16, ResNet, GoogleNet, and Inception ResNet for extraction and classification	88.00	9.00	15.00
5	Lenin G. [33] (2020)	(CBIS-DDSM), CLAHE for image enhancement, applied transfer learning/finetuning for VGG, ResNet, NasNet, DenseNet, Inception, MobileNet, Xception, and ResNext for feature extraction and classification.	81.58	21.73	15.10
6	Zeiser FA [28] (2020)	(CBIS-DDSM), CLAHE for enhancement and UNET models for feature extraction and classification.	85.95	7.68	19.53
7	Rose j [34] (2022)	(Mini-MIAS), region growing methods for segmentation and mobilenet for feature extraction and variational autoencoder for classification.	86.26	6.49	22.32

Breast mass classification using low-resolution mammograms can result in inaccurate results due to the limited information available. More relevant features are needed to address this to improve classification accuracy and reduce the number of FN and FP. High-resolution mammograms can be used to extract more detailed features that can be incorporated into the models to enable them to make more accurate decisions. Ultimately, this can lead to more accurate breast mass classification and better patient outcomes.

Super-resolution images obtained using different techniques have a broad spectrum of potential uses in healthcare. These images are able to refine the spatial granularity and quality of medical images, making them more accurate and reliable for diagnostic and treatment purposes. A few papers which used different techniques to generate super-resolution are specified below.

2.1. Models to Generate Super-Resolution Images

In 2014 Zheng J et al. [13] Authors designed an algorithm to generate high-resolution images, in which the first step is to align and register DDSM mammograms using a mesh warping algorithm. Then in the second step combination of a comprehensive model based on PCA and a local model utilizing patches can be used to generate HR images. These HR images are compared with HR images obtained with the nearest neighbor and bilinear, and the calculated PSNR values are 35.74, 31.56 and 32.57, respectively.

In 2017 Umehara K et al. [14], Authors trained the SRCNN and used it to generate HR mammograms from LR mammograms. They also generated HR mammograms using nearest neighbor and bilinear interpolations and compared them with HR mammograms generated from SRCNN. The PSNR of SRCNN, nearest neighbor, and bilinear interpolation are 34.50 ± 3.44 dB, 33.12 ± 3.18 dB, and 33.78 ± 3.34dB. So SRCNN produced images with improved resolution compared to traditional methods, which could be a useful tool for enhancing the diagnostic accuracy of mammograms.

In 2021 Shahidi F.[15] The paper presents a process to improve the spatial granularity of BC histopathology images using WA-GAN, which uses two loss functions, Wasserstein gradient penalty and perceptual loss, to improve the performance of the GAN model. The model generated HR images of factors 2, 4, 8 and 16. In this, the PSNR and SSIM values for factor 2 images are high (28.74, 0.96).

In 2018. Korkinof D et al. [16] The authors tried to communicate that training GANs progressively will generate highly realistic images. They explored how much HR images can be produced by GANS and how to overcome the underlying instabilities inherent in training GANs.

In 2020 Wang Z et al. [17] The authors have introduced udGAN, which is acquired by replacing the skip-connection structure in GANs generator with an ultra-dense residual network. Due to this replacement, the udGAN, with its high

number of connections and added feature extraction capabilities, is particularly suited for handling the varying complexities found in image content. They applied udGAN for video satellite imagery datasets from kaggle. The PSNR and SSIM obtained are 34.53 and 0.93, respectively.

In 2020 Zhang M et al. [18] the authors presented SPGAN in which the focus was on each pixel of the generated SR image, i.e., the proposed approach does not compare fake and real images but compares each pixel of images. They applied this GAN on datasets like VGGFace2, celebA and many more—the PSNR and SSIM obtained by SPGAN 25.98 and 0.78.

In 2022 Davradou A et al. [19] The authors presented the ISR model, which combines the techniques from SRGAN and ESRGAN and is used to generate high-resolution images of the foot of diabetic patients and to reduce noise in the foot images to monitor foot ulcers. They also used SRGAN, ESRGAN and EDSR to compare results with their model. The PSNR and SSIM values achieved by ISR are 45 and 0.95.

The focus of most papers on high-resolution (HR) image generation has been on enhancing image quality; very few studies have explored the potential applications of HR images. In response, a proposal has been made to utilize HR mammograms to reduce FNR and FPR in breast mass classification. By extracting more detailed and comprehensive features from HR images, the aim is to develop more accurate models for classification that can ultimately lead to better patient outcomes. The study seeks to bridge the gap between HR image generation and its practical applications in improving medical diagnosis and treatment.

2.2. Techniques to Enhance Images

In[20], histogram equalization, histogram stretching and median filters were used to enhance the mammograms. In [35], the authors used LCM-CLAHE to enhance mammograms. In order to overcome the loss of local information due to over-enhancement using CLAHE, they proposed LCM-CLAHE, which provides optimal contrast without losing much local information. In [22], the authors used NSCT as a part of the preprocessing step. To enhance the quality of breast lesions. A fuzzy-driven-based SR technique was implemented to predict intricate structures and detailed patterns accurately and to remove distortions after identifying the region of interest. In [23], authors used a combination of CLAHE and morphology methods to enhance mammograms so that the noise that remained in the mammogram after applying CLAHE could be removed by the morphology methods. In [24], authors used FC-CLAHE to enhance mammograms. In CLAHE, the clip value is fixed. Due to this, all pixel values in the image will be equally affected, which may not give a good contrast to the image. The authors have developed some fuzzy rules, using which the clip limit will be selected based on the data present in a mammogram. This method has enhanced image more than CLAHE. In [25], the authors used a pre-trained model DnCNN to enhance the mammograms, as it is pre-trained based on the previous learning it will enhance the images. In [26] this paper, the authors proposed a new CAD system in which mammograms are enhanced using CLAHE because AHE will over-enhance the noise in the images; next, mammograms are segmented with a region-based segmentation method. The segmented mammograms are given to the AlexNet model with an SVM classifier to extract features and classify masses. In [27], the authors used YOLO to detect masses, CLAHE for enhancing mammograms, full resolution convolutional network for mass segmentation and CNN for extraction of features and classification. In [28], the authors used CLAHE to enhance mammograms and U-Net for extraction and classification. In [31], the authors used filtering techniques and histogram equalization for preprocessing mammograms, autoencoder for feature extraction, RFE for feature reduction and various DL models for classification.

Throughout this discussion, various models that generate super-resolution images and techniques to enhance images have been explored. Combining SR techniques with enhancement can give scope to models to extract more relevant features from images and help in taking the right decisions. In this work, SRGAN is used to enhance the mammograms, extracting more detailed features from high-resolution images and ultimately improving breast mass classification accuracy by reducing FPR and FNR.

3. Proposed Approach

The proposed approach utilizes SR images to detect mammograms to reduce FP and FN. By using SR technology, the resolution of mammogram images was enhanced, which resulted in more accurate detection of abnormalities. This innovative approach aims to improve the accuracy of mammogram detection and ultimately save lives. The steps in the proposed model are presented in this section.

3.1. Datasets

CBIS-DDSM is the subset of DDSM, which is a dataset of mammograms with annotations for abnormalities such as masses and calcifications. It is a publicly available collection of mammography cases provided by the Cancer Imaging Archive. The CBIS-DDSM dataset includes both craniocaudal (CC) and mediolateral oblique (MLO) views of the breasts, with a total of 1697 images. Of these images, 909 are benign, and 788 are malignant. The images are in dicom format and have been carefully curated and annotated by expert radiologists. The CBIS-DDSM dataset is commonly used to develop and evaluate ML methods for mammogram analysis, aiming to improve the accuracy and efficiency of a breast cancer diagnosis.

The Mini-MIAS dataset collects 323 mammograms, including 207 normal, 64 benign, and 52 malignant cases. It

was generated by the MIAS group in the UK and published in 1994. The mammograms in the Mini-MIAS dataset are all in the mediolateral oblique (MLO) view and are in the PGM format. The Mini-MIAS dataset is often used to develop and evaluate ML techniques for mammogram analysis, aiming to improve the accuracy and efficiency of a breast cancer diagnosis. Because the dataset is relatively small and only includes MLO views, it is often used as a supplementary dataset alongside larger and more diverse datasets, such as the CBIS-DDSM and INbreast datasets. The INbreast dataset is a collection of mammograms from 115 cases, with a total of 410 images.

It includes mammograms in both CC and MLO views and depicts various abnormalities such as masses, calcifications, asymmetries, and distortions. Of the 410 mammograms in the dataset, 108 are related to masses. The mammograms are in dicom format and have varying resolutions. The INbreast dataset is commonly used to develop and evaluate ML techniques for mammogram analysis, aiming to improve the accuracy and efficiency of a breast cancer diagnosis. It is a useful resource for researchers due to its diverse range of abnormalities and views and its larger size compared to the Mini-MIAS dataset.

3.2. Image Preprocessing

Image preprocessing is an essential step in the analysis of medical images, as it can help to enhance the quality and clarity of the images and improve the performance of subsequent ML and DL methods. Mammograms from CBIS-DDSM, Mini-MIAS and INbreast are combined. The combined data is divided into 2 sets, CC views and MLO views. In the first step of the proposed approach, artifacts are removed from mammograms; in the second step, pectoral muscle is removed from mammograms. Masses are segmented using thresholding techniques.

3.3. Segmentation

Thresholding is a process in image processing that involves dividing an image into two or more classes (foreground and background) based on the intensity values of the pixels. It is often used to segment objects in an image by setting a threshold value and assigning all those with values above a certain limit(threshold) are assigned to one class, and those with values below the limit are assigned to another class. The thresholding techniques are used to extract mass from super-resolution mammograms and high-resolution mammograms.

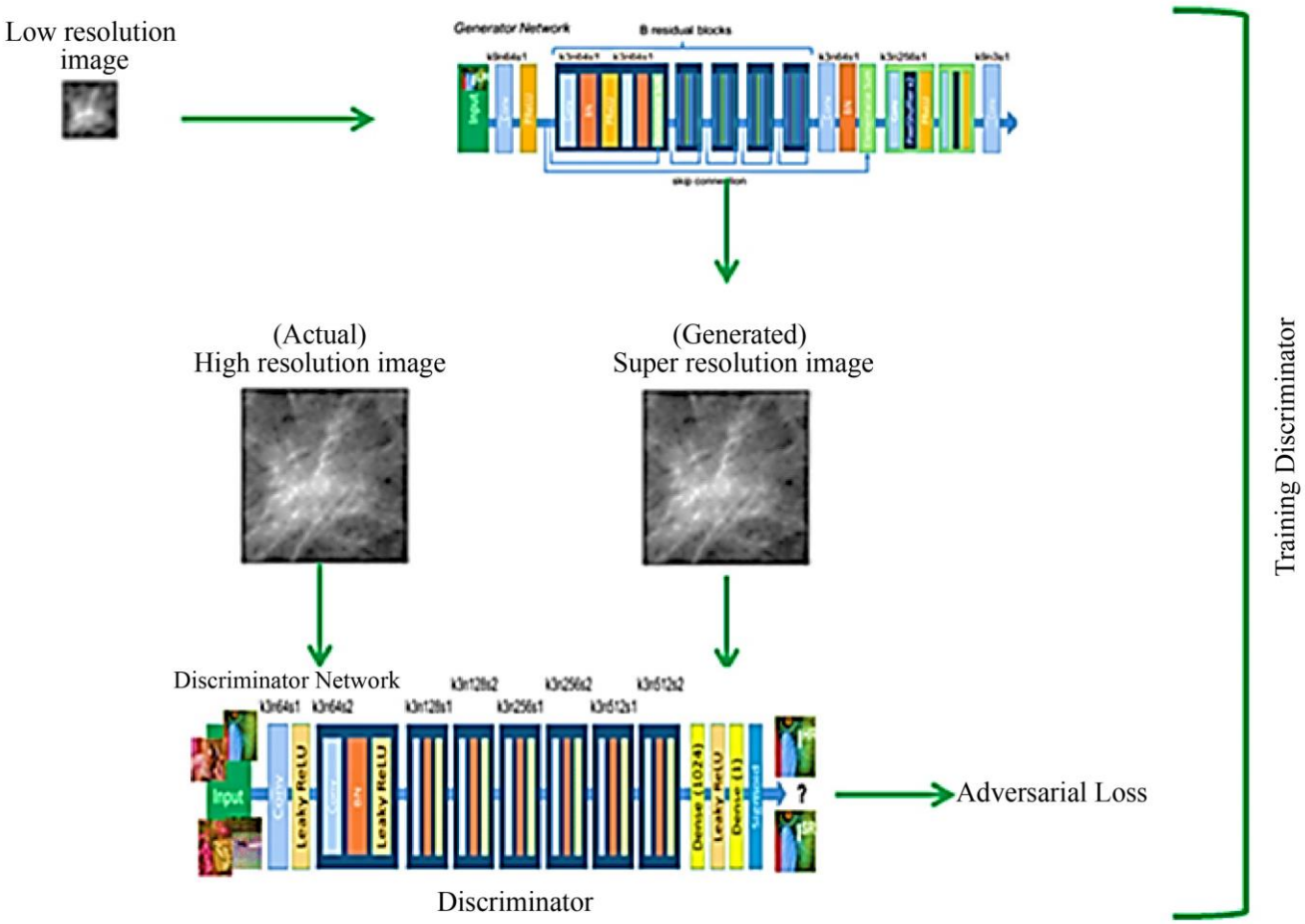

Fig. 1 Architecture for training discriminator

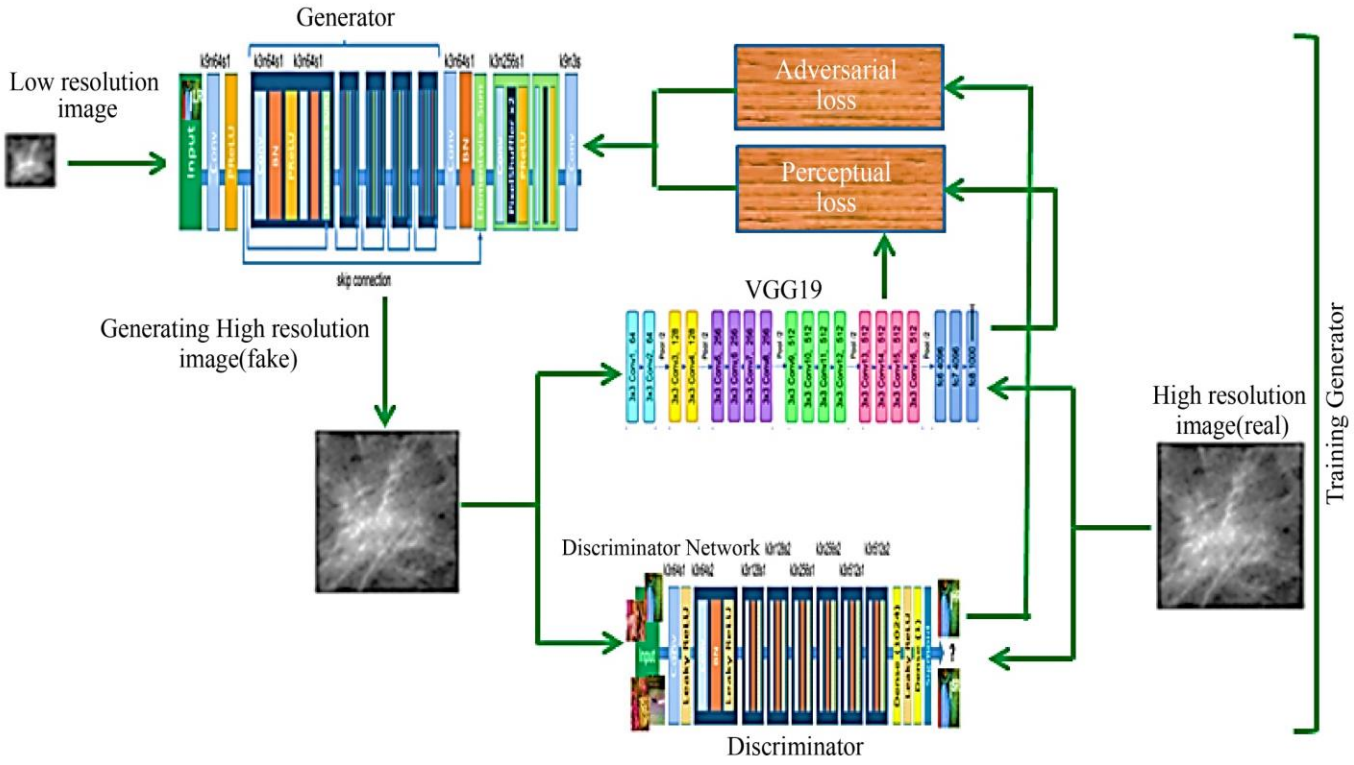

Fig. 2 Architecture for training generator

3.4. SRGAN

The GAN provides a novel approach to generating images and serves as a foundation for building high-resolution image models. SRGAN [8] has introduced a generative adversarial network into super-resolution, which has acquired superior visual clarity and realism in the finely-detailed image with intricate features and nuances. SRGAN mainly consists of two sections generator and a discriminator. HR images and generated HR images are given to SRGAN during training, as presented in Fig. 1. Generator generates HR images from LR images and passes these generated images to the discriminator. Discriminator distinguishes the generated HR images from the original HR images and the adversarial loss is computed. The perceptual loss is calculated on feature maps of the VGG network. This combined loss is passed to the generator, as shown in Fig. 2.

The architecture of SRGAN is coded as in [8]. 16 residual blocks are used in the generator; the features of images are extracted from the 10th layer of the VGG19. To obtain super-resolution images from SRGAN, it has been trained with 32X32 LR images and 128X128 HR images for 100 epochs, with Adam optimizer and learning rate 10^{-4}. The quality of super-resolution images is measured with PSNR and SSIM measures. PSNR, which stands for Peak Signal-to-Noise Ratio, is a metric used to evaluate the fidelity of a reconstructed image in comparison to the original image. This measure is obtained by dividing the maximum power that a signal can achieve by the power of the noise or error that has been introduced during the transmission of the image. Structural Similarity Index Measure (SSIM) is a method used to calculate the similarity between two images. The findings (PSNR and SSIM results) show that the super-resolution images contain significantly more high-frequency information compared to images generated by traditional methods. High-resolution images are generated using SRGAN.

3.5. Augmentation

As mammograms are medical images, the DL models may use the size and shape of the mass in diagnosing breast cancer, so only specific augmentation techniques are used. The numbers of benign mammograms are 1006, and malignant is 888. Every image in the dataset is rotated in [20, 40, 60, 80, 120, 140, 160, 180, 200, 220, 240, 260, 280, 300, 320, 340], shifted vertically and horizontally. Super-resolution images are augmented after augmentation total number of images is around 37,940.

3.6. EfficientNet Models

The architecture of EfficientNet[30] models is based on combining a few key ideas: compound scaling, depthwise separable convolutions and Squeeze-and-excitation blocks. Compound scaling is a method of scaling up the model's dimensions by a fixed scaling coefficient. This scaling coefficient, denoted as "alpha," is used to scale up all model dimensions uniformly. The goal of compound scaling is to maintain a good balance between representation capacity and computational cost as the model scales up. It allows the model

to improve its performance on a given task by increasing the capacity of the model while simultaneously controlling the computational cost. Table 2. presents the scaling of EfficientNet models.

To enhance the efficiency of a model, depthwise separable convolutions are employed. These convolutions utilize a technique that breaks down a conventional convolution into two distinct operations: a depthwise convolution and a pointwise convolution. The depthwise convolution operates on each input channel independently, applying a different filter to each channel. This can be implemented efficiently using a single convolutional kernel with a shape that is the same as the input channel size (e.g., 3x3 for an input with 3 channels). The depthwise convolution has a computational cost that is linear in the number of input channels, making it much more efficient than a standard convolution, which has a cost that is quadratic in the number of input channels.

The pointwise convolution combines the output of the depthwise convolution using a set of 1x1 convolutional kernels. This allows the model to learn more complex relationships between the input channels. The pointwise convolution has a linear computational cost in the number of input and output channels, making it more efficient than a standard convolution, which has a quadratic cost in the number of input and output channels. Overall, depthwise separable convolutions are able to achieve good performance with significantly fewer parameters and FLOPS compared to standard convolutions in Fig 3. Sections 3 and 6 are for depthwise and pointwise convolutions.

Squeeze-and-excitation (SE) functions are a type of attention mechanism that can be used to improve the performance of convolutional neural networks. The idea behind SE functions is to use a "squeeze" operation to aggregate the spatial information from all channels at each position in the feature map and an "excitation" operation to use this aggregated information to weight the channels at each position. This allows the model to adaptively re-calibrate the feature maps and improve the representation power of the model. In Fig. 3, section 5 is for SE.

Skip connections in the EfficientNet models allow information to bypass one or more layers in the neural network, effectively allowing the network to learn a shortcut that can improve the flow of information and ultimately improve the model's accuracy. This can also help to reduce the risk of overfitting by allowing the model to access lower-level features more easily. All these features made EfficientNet models more robust and highly efficient. In Fig.3, the layer Add is for skip connections. Fig. 4 represents the architecture of the EfficientNetB0 model.

3.7. Transfer Learning

Transfer learning in deep learning models involves utilizing pre-trained neural networks as a starting point for a new task rather than training a model from scratch. This approach leverages the knowledge acquired during the training of the original model, allowing for faster convergence and improved performance on the new task. Knowledge transferability depends on the degree of similarity between the new task and the task for which the pre-trained model was trained. This technique is particularly useful for tasks with limited data availability, as it allows for the utilization of large amounts of pre-existing data to improve the new model's performance.

There are several benefits of using transfer learning in deep learning models:

- Faster convergence: By starting with a pre-trained model, the training process can converge faster, as the model already has a good understanding of the underlying features in the data.
- Improved performance: Transfer learning can improve the new model's performance, as it allows the model to leverage the knowledge acquired during the training of the original model.
- Handling limited data availability: Transfer learning is particularly useful for tasks with limited data availability, as it allows the utilization of large amounts of pre-existing data to improve the new model's performance.
- Wide range of applications: Transfer learning has been shown to be effective in various fields such as NLP, CV and speech recognition.
- Cost-effective: Using pre-trained models can save time and resources, as the model has already been trained on a large dataset. This makes it more cost-effective than training a model from scratch.
- Reusability: Pre-trained models can be reused multiple times, which makes it more efficient in terms of time and resources.

Transfer learning was applied in training EfficientNet Models with SR mammograms.

3.8. The Proposed Model

The proposed model aims to improve upon traditional breast cancer detection methods by using deep learning techniques to extract more relevant features from medical images, specifically mammograms. Instead of using features from a general image database (Imagenet), this model uses features from a medical image database specifically for mammograms. Additionally, the model uses features extracted from convolutional layers, which have a wider range of feature extraction capabilities, rather than dense layers. By training the last few layers of the deep learning model using a mammogram dataset, the model can learn features specific to mammogram masses.

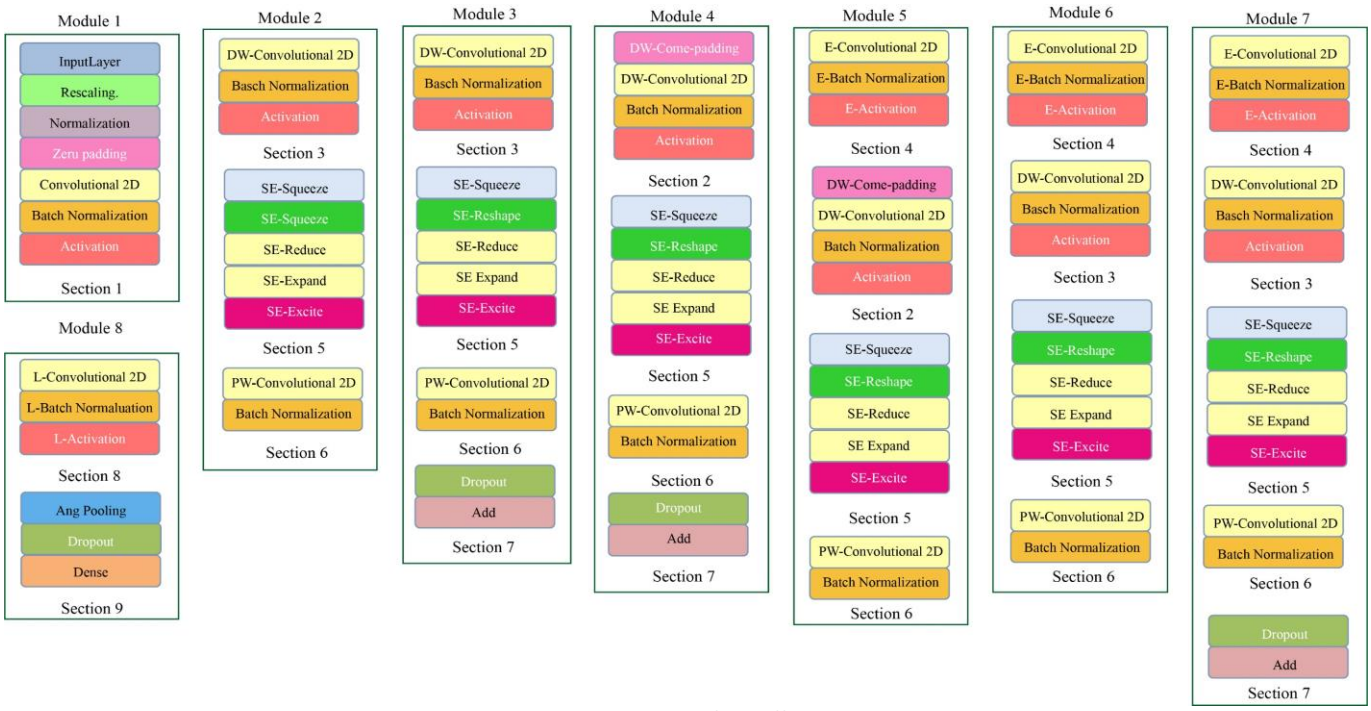

Fig. 3 Sections and modules of the EfficientNet model

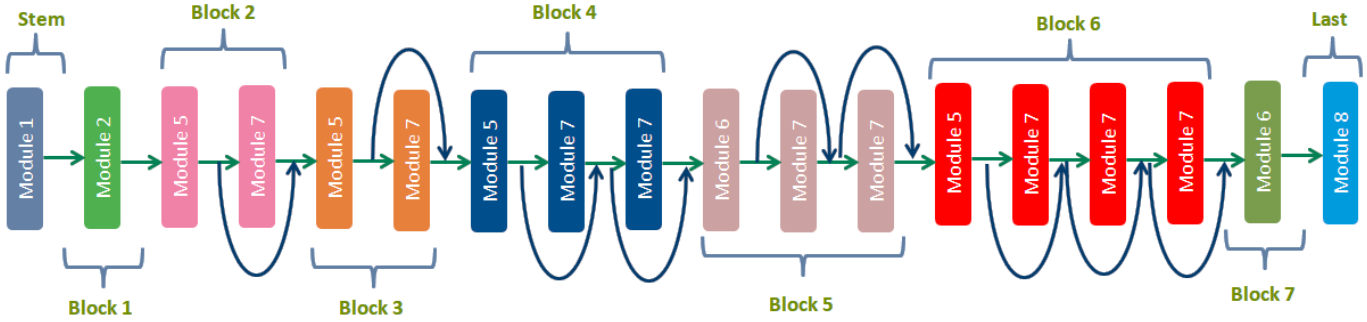

Fig. 4 Architecture of EfficientNetB0 model

Table 2. Architecture details of EfficientNet Models

Model/ Block	Family of EfficientNet Models						
	B0	**B1**	**B3**	**B4**	**B5**	**B6**	**B7**
Stem	Module 1	Module 1	Module 1	Module 1	Module 1	Module 1	Module 1
Block1	Module 2	Module 2	Module 2	Module 2	Module 2	Module 2	Module 2
		Module 3	Module 3	Module 3	Module 3x2	Module 3x2	Module 3x3
Block2	Module 5	Module 5	Module 5	Module 5	Module 5	Module 5	Module 5
	Module 7	Module 7x2	Module 7x2	Module 7x3	Module 7x4	Module 7x5	Module 7x6
Block3	Module 5	Module 5	Module 5	Module 5	Module 5	Module 5	Module 5
	Module 7	Module 7x2	Module 7x2	Module 7x3	Module 7x4	Module 7x5	Module 7x6
Block4	Module 5	Module 5	Module 5	Module 5	Module 5	Module 5	Module 5
	Module 7x2	Module 7x3	Module 7x4	Module 7x5	Module 7x6	Module 7x7	Module 7x9
Block5	Module 6	Module 6	Module 6	Module 6	Module 6	Module 6	Module 6
	Module 7x2	Module 7x3	Module 7x4	Module 7x5	Module 7x6	Module 7x7	Module 7x9
Block6	Module 5	Module 5	Module 5	Module 5	Module 5	Module 5	Module 5
	Module 7x3	Module 7x4	Module 7x5	Module 7x7	Module 7x8	Module 7x10	Module7x12
Block7	Module 6	Module 6	Module 6	Module 6	Module 6	Module 6	Module 6
		Module 7	Module 7	Module 7	Module 7x2	Module 7x2	Module 7x3
Last	Module 8	Module 8	Module 8	Module 8	Module 8	Module 8	Module 8

One potential solution to the limited data problem in medical image analysis is to augment available datasets and combine them to create a larger training set. This approach, known as multi-dataset training, helps increase the robustness and generalizability of the model. However, in mammography, the small size of masses captured in images can lead to loss of detail and introduction of artifacts when the masses are resized for input into a deep learning model.

GAN (SRGAN) was used to generate super-resolution images of the masses to address this issue. These images have a higher pixel density and more detailed information, which can increase the model's accuracy by reducing false negatives and false positives. The increased resolution of the training images allows the model to identify better and classify the features present in the image.

Fig.5 presents a flow chart of the proposed approach, and Fig.6 presents the architecture of the proposed model. Algorithm provides a succinct overview of the model's process.

4. Experiments and Results

In this paper, to improve the resolution and clarity of preprocessed mammograms, first mammograms are used to train the super-resolution generative adversarial network (SRGAN) model. The model is trained with 7965 images for 100 epochs; a model is saved for every 10 epochs. The models are evaluated and computed PSNR and SSIM values which are presented in Table 3.

The 100 epoch model values suggest the image quality is relatively high, as both(PSNR and SSIM) values are relatively close to the maximum possible value of 50 for PSNR and 1 for SSIM. The trained SRGAN model was then utilized to generate high-resolution mammograms of size 600X600. The generated SR images are enhanced and augmented and then applied to EfficientNet models.

Transfer learning with finetuning is applied on all EfficientNet Models; all the layers in the last 3 blocks of every EfficientNet model(block 5, block 6, block 7) are trained. The list of layers trained in EfficientNet models is presented in Table 4. Every EfficientNet model is trained with 70% of the data, validated with 10% of the data and evaluated with 20% of the data. Every model is trained for 20 epochs with batch size ranging from 4-16, 'Adam' optimizer and learning rate(lr) 10^{-4}

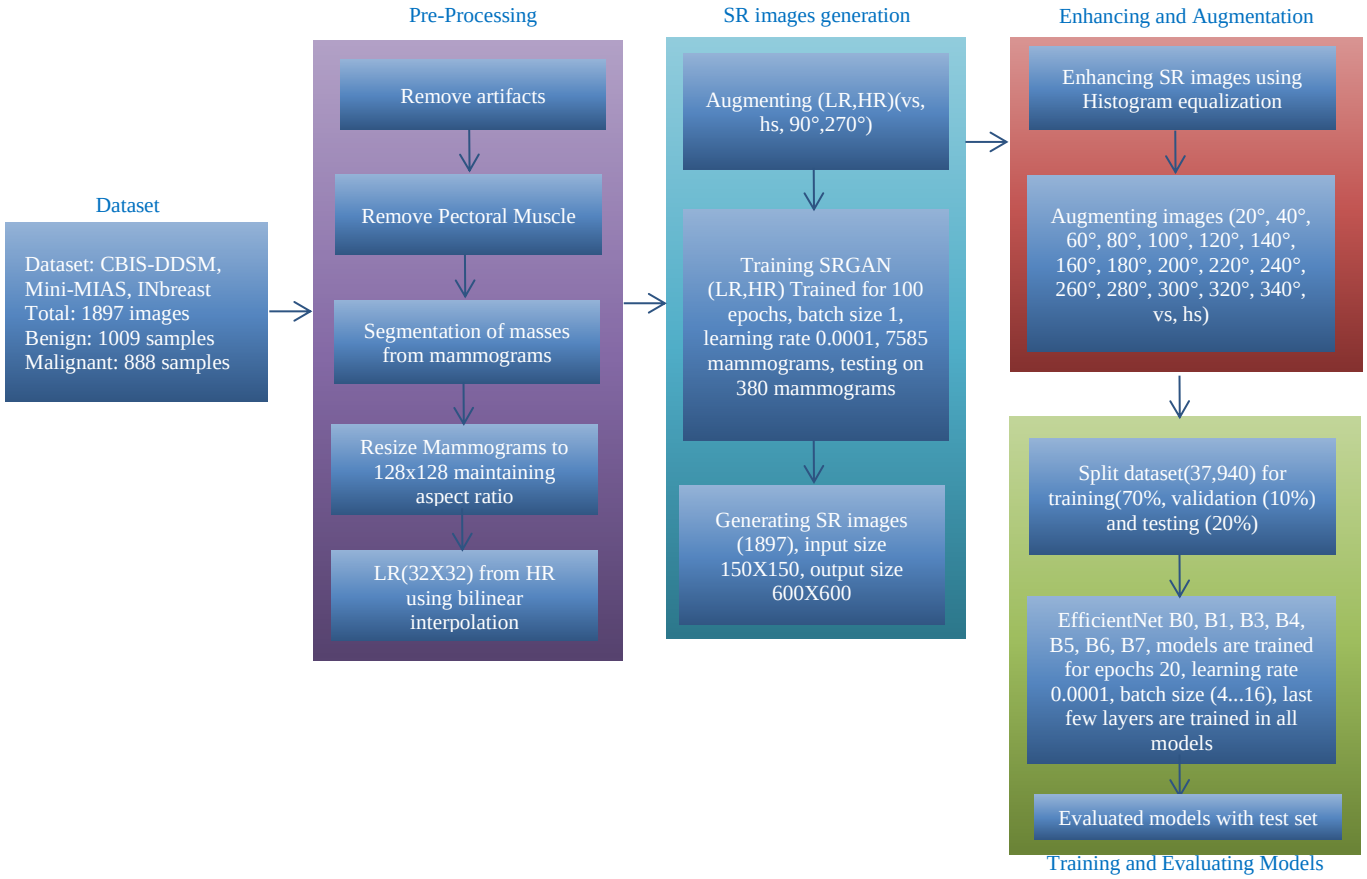

Fig. 5 Flowchart for the proposed model

Algorithm: SRGAN with EfficientNet to reduce FPR and FNR

rt-removal of artifacts, pm-removal of the pectoral muscle, rs-resize, seg-segmentation, he-histogram equalization, aug-augmentation, m-model, (d1, d2, d3, ... are datasets in different stages in the preparation of dataset to train the model)
Input: Dataset- [CBIS-DDSM, Mini-MIAS, INbreast mammograms]
Output: [confusion matrix, accuracy, precision, recall, specificity]
Step 1: Load Dataset
Step 2: Preprocessing of Dataset
    2.1: d1 = rt (Dataset)
    2.2: d2 = pm(d1)
Step 3: Segmentation of mass
    3.1: d3 = seg(d2)
Step 4: LR and HR images
    4.1: HR = rs(d3)
    4.2: LR = rs(HR)
Step 5: Process to get super-resolution images
    5.1: m = training (SRGAN, LR, HR)
    5.2: sr = m(d3) //sr dataset of super-resolution images
Step 6: Process to enhance images
    6.1: hsr = he(sr)
Step 7: Augmentation
    7.1: augs = aug(hsr)
Step 8: split dataset(augs) for training, testing and validation
Step 9: train pretrained models (efficientnetb0, b1, b3, b4, b5, b6, b7)
    9.1: finetune model parameters (freezing, training layers, epochs, learning rate, batch size)
    9.2: testing the models
Step 10: compute [confusion matrix, accuracy, precision, recall, specificity]
Step 11: evaluation and analysis

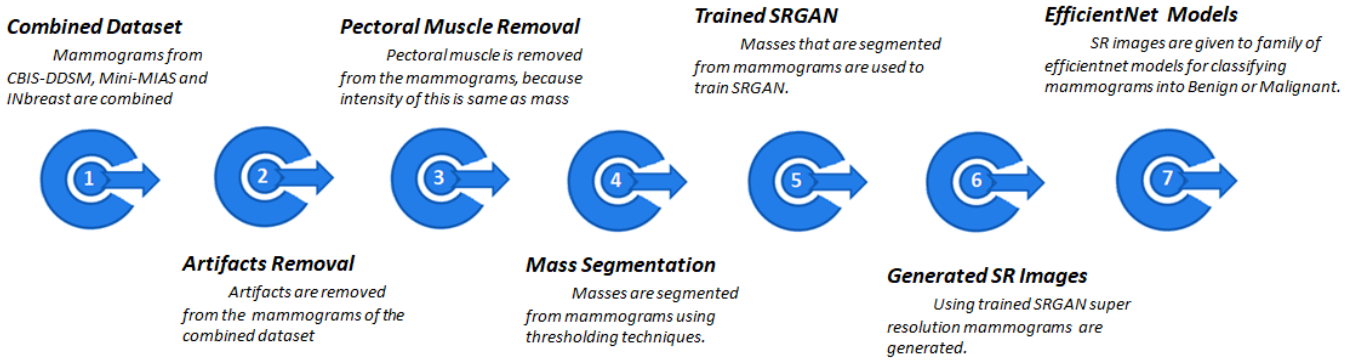

Fig. 6 Architecture of the proposed model

4.1. Comparing the Family of EfficientNet Model's Performance in Reducing False Negatives

One of the points that the present study focused on was minimizing the rate of false negatives in breast cancer detection. The values in Table 5 and the graph in Fig.8. illustrate the rate of false negatives achieved by the family of EfficientNet Models with high-resolution images obtained from SRGAN(SM); The findings reveal a consistent reduction in false negatives as the combination of SM with EfficientNet models advanced from the less complex EfficientNetB0 to the more sophisticated EfficientNetB7.

This trend suggests that the higher capacity models within the EfficientNet family can extract more relevant features effectively from the SR images, leading to a high accuracy rate in the classification of breast cancer cases. The observed improvement in the rate of false negatives indicates the higher capability of the EfficientNet models in identifying cases that may have been missed by lower capacity models, potentially leading to improved patient outcomes and early detection of breast cancer. Fig.10 presents the confusion matrix of EfficientNetB0 to EfficientNetB7 models.

Table 3. PSNR and SSIM values obtained by the SRGAN model

No. of Epochs	PSNR	SSIM
10	16.51	0.62
20	19.46	0.72
30	23.99	0.73
40	26.73	0.78
50	28.33	0.84
60	29.21	0.85
70	30.34	0.85
80	32.63	0.86
90	34.22	0.86
100	36.52	0.87

Table 4. The layers trained in EfficientNet models

Model	No. of layers	Starting Layer	No. of layers trained
EfficientNetB0	237	120	118
EfficientNetB1	339	177	163
EfficientNetB3	384	192	193
EfficientNetB4	474	237	238
EfficientNetB5	576	294	283
EfficientNetB6	666	339	328
EfficientNetB7	813	411	403

Table 5. Results obtained by EfficientNet models

	Super Resolution Images		
Models	**Accuracy %**	**False Negative Rate**	**False Positive Rate**
EfficientNetB0	98.69	0.0110	0.0160
EfficientNetB1	99.24	0.0061	0.0093
EfficientNetB3	99.29	0.0078	0.0063
EfficientNetB4	99.39	0.0075	0.0048
EfficientNetB5	99.53	0.0038	0.0056
EfficientNetB6	99.65	0.0032	0.0039
EfficientNetB7	99.71	0.0029	0.0029

Table 6. Results obtained by EfficientNet Models

	Super Resolution Images		
Models	**Accuracy %**	**Recall %**	**Precision %**
EfficientNetB0	98.69	98.94	98.59
EfficientNetB1	99.24	99.39	99.19
EfficientNetB3	99.29	99.22	99.45
EfficientNetB4	99.39	99.25	99.49
EfficientNetB5	99.53	99.62	99.50
EfficientNetB6	99.65	99.68	99.62
EfficientNetB7	99.71	99.75	99.71

4.2. Comparing the Family of EfficientNet Model's Performance in Reducing False Positives

The other point which present study focused on was minimizing the rate of false positives in breast cancer detection. The graph in Fig.7 and the values in Table 5. illustrates the rate of false positives achieved by the family of EfficientNet Models with high-resolution images obtained from SRGAN(SM). The results demonstrate a consistent reduction in false positives as it progresses from EfficientNetB0 to EfficientNetB7 when combined with SR images. This trend suggests that the higher capacity models within the EfficientNet family are able to extract more relevant features effectively from the SM, leading to a high accuracy rate in the classification of breast cancer cases. The observed improvement in the rate of false positives indicates the higher capability of the EfficientNet models in identifying cases that may have been missed by lower capacity models, potentially leading to improved patient outcomes and early detection of breast cancer. Fig.10 presents Confusion matrices of EfficientNetB0 to EfficientNetB7 models.

4.3. Comparing the Family of EfficientNet Model's Performance in Increasing Accuracy

Incorporating EfficientNet models in the analysis of super-resolution mammograms resulted in a substantial decrease in both false positive and false negative rates, thereby illustrating a significant improvement in diagnostic accuracy. Fig.9 gives the rate of loss and accuracy obtained by EfficientNetB7 when it was trained. Table 6 presents the accuracy, precision and recall achieved by EfficientNetB0 to B7 and a graphical representation is presented in Fig.11; Table 7 and Table 8 present the results in comparison with the proposed system to previous research. The false positive and false negative rate acheived by our proposed model is 0.0029, which is almost equal to zero, and the accuracy achieved is 99.71%.

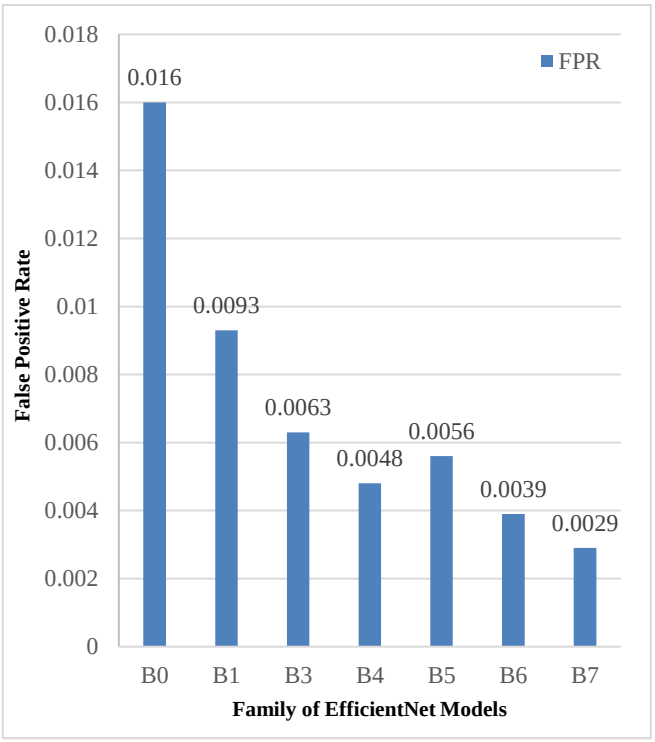

Fig. 7 False positive rate obtained by EfficientNet models

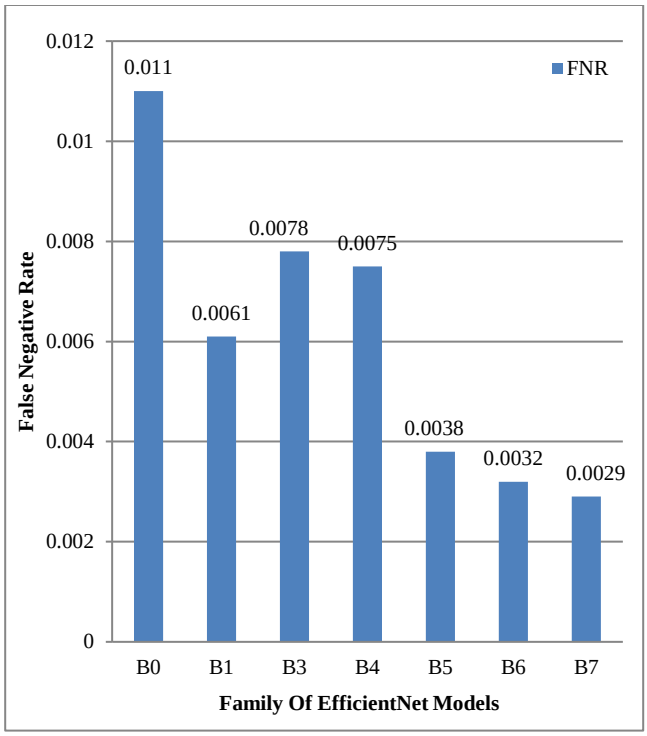

Fig. 8 False negative rate obtained by EfficientNet models

4.4. Overall Analysis

Upon applying super-resolution images to the family of EfficientNet models, which possess a high degree of scalability, have shown a progressive increase in accuracy and a concomitant decrease in false negatives and false positives. This balanced optimization of performance metrics was not consistently replicated when utilizing other model architectures. This can be attributed to the unique design principles and optimization techniques employed in the EfficientNet models, which enable a more finely tuned and holistic enhancement of model performance.

The EfficientNet models demonstrate a superior ability to learn complex image features robustly and effectively, resulting in a more consistent and reliable improvement in results. Selecting an appropriate model for a given task is crucial for achieving optimal performance. The characteristics of the data, such as its size, type, and distribution, must be carefully considered when selecting a model, which can lead to superior performance and yield valuable insights from the data.

4.5. Strategies Employed to Reduce FPR and FNR in this Research

Several strategies were employed to reduce and balance the FPR and FNR through the proposed model. Firstly, high-resolution images were used instead of low-resolution images to extract more relevant features for better decision-making. By doing this, more details could be extracted from the images, which could help the model make better decisions. Secondly, a GAN model, a powerful deep learning technique for image generation, was applied to produce high-quality super-resolution images that could provide more details to aid in making accurate decisions. GANs possess the capability to comprehend intricate patterns within image data and create lifelike images that are challenging to differentiate from genuine ones.

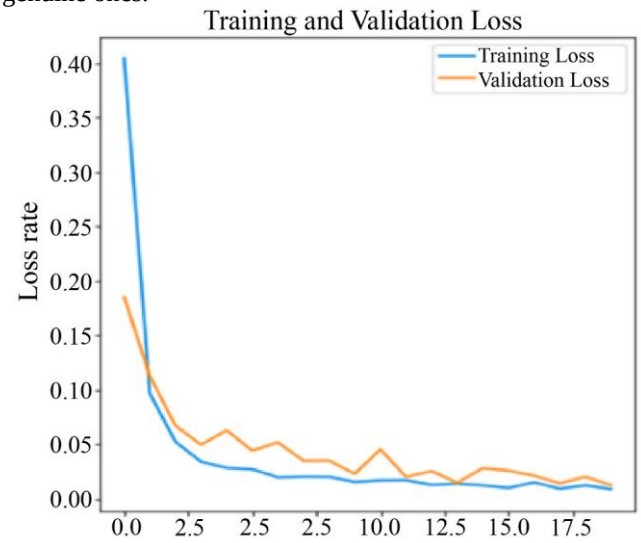

9(a)

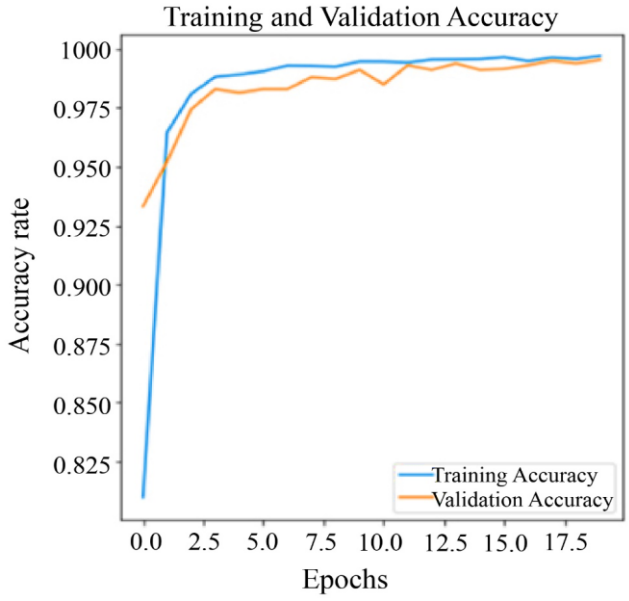

9(b)

Fig. 9 Presents the rate of (a) loss while training EfficientNetB7 (b) accuracy while training EfficientNetB7.

In addition to these strategies, the model's ability to generalize was enhanced by merging three distinct datasets The combination of different datasets provided a wider range of variations in the data, which helped the model to learn more robust and diverse features. Various transformations, such as flipping and rotating, were applied to augment the dataset and enhance the model's robustness. The quantity of training data is increased through the application of data augmentation.

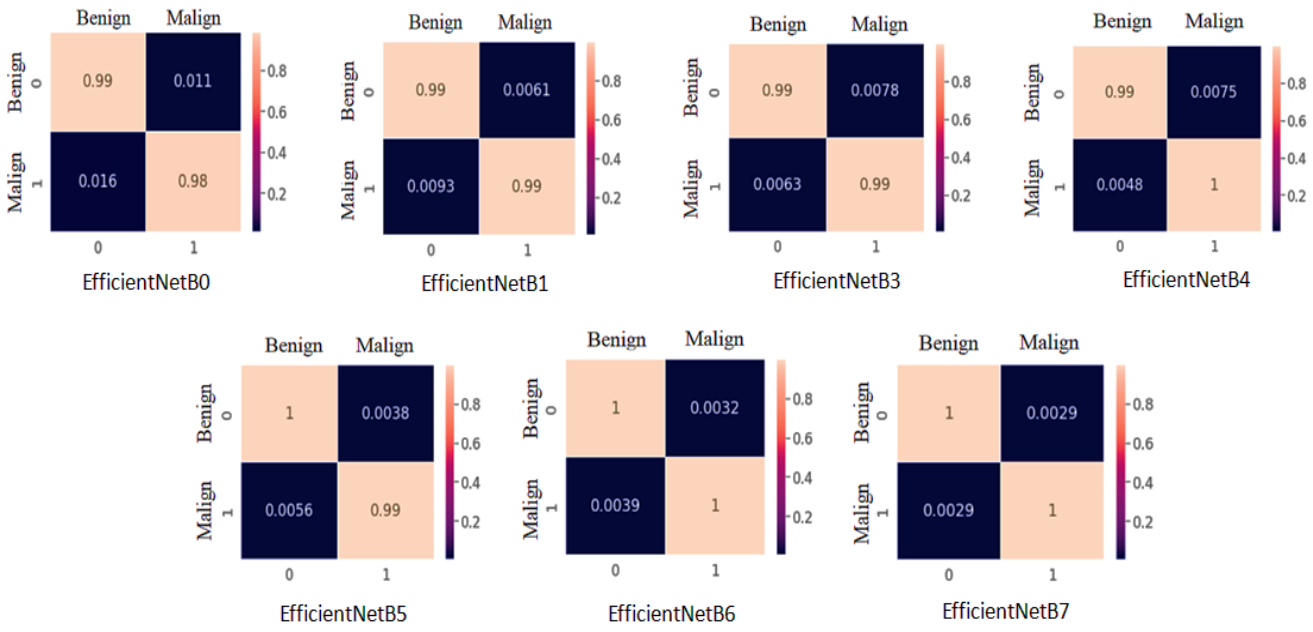

Fig. 10 Presents confusion matrices of all EfficientNet models from B0 to B7

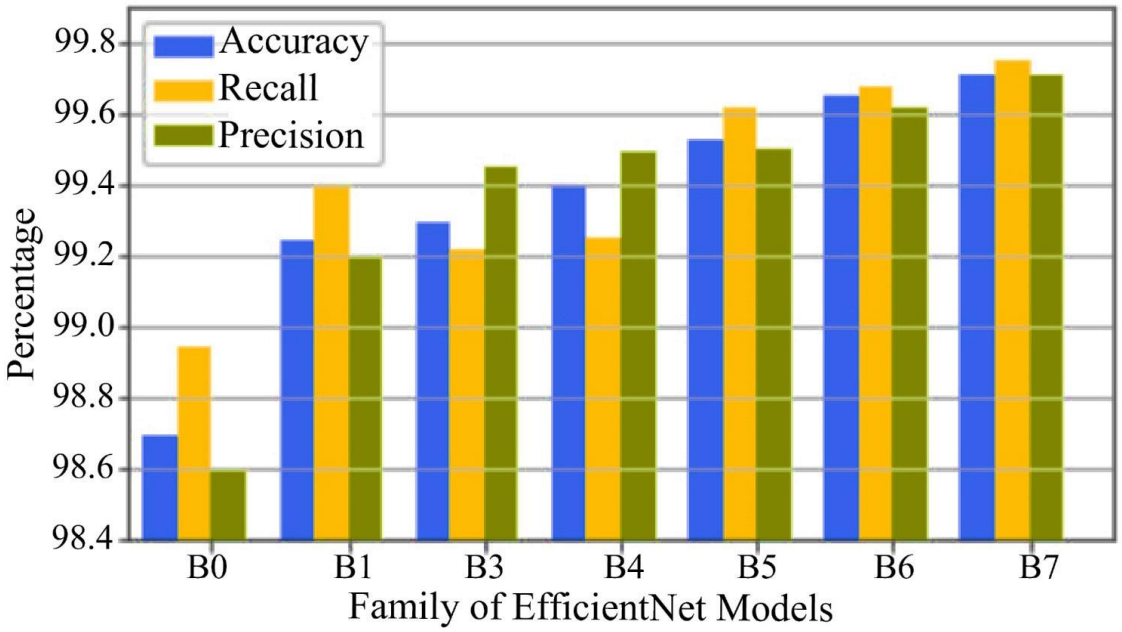

Fig. 11 Presents accuracy, precision, and recall obtained by all EfficientNet models from B0 to B7

Table 7. Presents accuracy, precision, and recall obtained by all EfficientNet models from B0 to B7

S.No	Article	Accuracy %	Sensitivity %	Specificity %
1	**Ragab DA [26]**	87.20	86.20	87.70
2	**Pak F [22]**	91.43	87.15	93.58
3	**Zeiser FA [28]**	85.95	92.32	80.47
4	**Al-Antari MA [27]**	95.64	97.14	92.41
5	**Pratheep Kumar P [31]**	96.00	97.00	98.00
6	**Proposed Model**	99.71	99.75	99.71

Table 8. Comparison of results with previous research in SR

S.No	Article	PSNR	SSIM/MSSIM
1	Zheng J [13]	35.74	0.81
2	Umehara K [14]	34.50 ± 3.44 dB	0.785 ± 0.103
3	Shahidi F [15]	28.74	0.96
4	Wang Z [17]	34.53	0.93
5	Zhang M [18]	25.98	0.78
6	Davradou A [19]	45.00	0.95
7	Proposed System	36.52	0.87

Available to the model, leading to improved performance and reduced overfitting.

To further improve the performance of the models, EfficientNet models were used to train the SR images. EfficientNet models comprise a group of NN devised to achieve state-of-the-art performance on image classification tasks with fewer parameters than traditional deep learning models. The EfficientNet models have a unique architecture that allows them to achieve high accuracy with a smaller number of parameters, making them more efficient and faster to train. By using EfficientNet models, higher accuracy was achieved in the models while keeping the number of parameters low.

Finally, the models were finetuned by tuning the hyperparameters after many experiments to achieve the best possible performance. The model's performance could be optimized by tuning the hyperparameters, and better results could be achieved. The last three blocks of every model were also trained to finetune the models further and achieve better results.

Overall, using high-resolution images, utilizing a GAN model, combining different datasets, augmenting the dataset, using EfficientNet models, and finetuning the models through hyperparameter tuning and last-block training, the FPR and FNR in the models were reduced and balanced.

5. Conclusion and Future Work

The present study aimed to reduce false negatives and false positives in the classification of mammograms using super-resolution images and deep learning techniques. To this end, an approach was proposed that used the capabilities of a GAN to synthesize SR images from a small, artifact-free dataset of mammograms.

The results demonstrated that the use of SR images, particularly when paired with the most effective medical image classification model, resulted in a significant reduction in false negatives and false positives. These findings suggest that using GAN-based super-resolution, combined with appropriate deep learning architectures, holds promise for improving the accuracy and reliability of mammogram analysis.

One potential approach to address the challenge of limited data availability in the medical image domain is to leverage the power of generative models, such as GAN. These models have the ability to synthesize highly realistic images by learning the underlying distribution of a given dataset. By training GANs on a small dataset of real medical images, it may be possible to generate a larger augmented dataset, which can be utilized to train DL models. This approach has the potential to greatly enhance the generalization capacity of the trained models and improve their performance on unseen data.

One important point is that the quality and realism of the synthesized images generated by GANs depend on the capacity and training of the model, as well as the diversity and complexity of the underlying dataset. Therefore, it will be crucial to carefully evaluate the effectiveness of different GANs for use in downstream tasks. This will be pursued in future initiatives.

References

[1] Alexey Lukin, Andrey S. Krylov, and Andrey Nasonov "Image Interpolation By Super-Resolution," *In Proceedings of Graphicon,* vol. 2006, pp. 239-242, 2006. [Google Scholar] [Publisher Link]

[2] R. Key, "Cubic Convolution Interpolation for Digital Image Processing," *IEEE Transactions on Acoustics, Speech, and Signal Processing*, vol. 29, no. 6, pp. 1153-60, 1981. [CrossRef] [Google Scholar] [Publisher Link]

[3] Chao Dong et al., "Image Super-Resolution Using Deep Convolutional Networks," *IEEE Transactions on Pattern Analysis and Machine Intelligence*, vol. 38, no. 2, pp. 295-307, 2016. [CrossRef] [Google Scholar] [Publisher Link]

[4] Chao Dong, Chen Change Loy, and Xiaoou Tang, "Accelerating the Super-Resolution Convolutional Neural Network," *In: European Conference on Computer Vision*, vol. 9906, pp. 391–407, 2016. [CrossRef] [Google Scholar] [Publisher Link]

[5] Wenzhe Shi et al., "Real-Time Single Image and Video Super-Resolution Using an Efficient Sub-Pixel Convolutional Neural Network," *In Proceedings of the IEEE Conference on Computer Vision and Pattern Recognition*, pp. 1874- 1883, 2016. [CrossRef] [Google Scholar] [Publisher Link]

[6] Jiwon Kim, Jung Kwon Lee, and Kyoung Mu Lee, "Accurate Image Super-Resolution Using Very Deep Convolutional Networks," *In Proceedings of the IEEE Conference on Computer Vision and Pattern Recognition*, pp. 1646- 1654, 2016. [CrossRef] [Google Scholar] [Publisher Link]

[7] Bee Lim et al., "Enhanced Deep Residual Networks For Single Image Super- Resolution," *In Proceedings of the IEEE Conference on Computer Vision and Pattern Recognition Workshops*, pp. 136-144, 2017. [CrossRef] [Google Scholar] [Publisher Link]

[8] Christian Ledig et al., "Photo-Realistic Single Image Super-Resolution Using a Generative Adversarial Network," *In Proceedings of the IEEE Conference on Computer Vision and Pattern Recognition*, pp. 4681-4690, 2017. [CrossRef] [Google Scholar] [Publisher Link]

[9] Xintao Wang et al., "Esrgan: Enhanced Super-Resolution Generative Adversarial Networks," *Inproceedings of the European Conference on Computer Vision (ECCV) Workshops*, pp. 1-16, 2018. [Google Scholar] [Publisher Link]

[10] Alec Radford, Luke Metz, and Soumith Chintala, "Unsupervised Representation Learning with Deep Convolutional Generative Adversarial Networks," *Arxiv Preprint Arxiv:1511.06434*, 2016. [CrossRef] [Google Scholar] [Publisher Link]

[11] Mehdi Mirza, and Simon Osindero, "Conditional Generative Adversarial Nets," *Arxiv Preprint Arxiv:1411.1784*. 2014. [CrossRef] [Google Scholar] [Publisher Link]

[12] Martin Arjovsky, Soumith Chintala, and Léon Bottoul, "Wasserstein Generative Adversarial Networks," *International Conference on Machine Learning*, vol. 70, pp. 214-223, 2017. [Google Scholar] [Publisher Link]

[13] Jun Zheng, Olac Fuentes, and Ming-Ying Leung, "Super-Resolution of Mammograms," *In 2010 IEEE Symposium on Computational Intelligence In Bioinformatics and Computational Biology*, pp. 1-7, 2010. [CrossRef] [Google Scholar] [Publisher Link]

[14] Kensuke Umeharaorcid, Junko Ota, and Takayuki Ishida, "Super-Resolution Imaging of Mammograms Based on the Super-Resolution Convolutional Neural Network," *Open Journal of Medical Imaging*, vol. 7, no. 4, 2017. [CrossRef] [Google Scholar] [Publisher Link]

[15] Faezehsadat Shahidi, "Breast Cancer Histopathology Image Super-Resolution Using Wide-Attention Gan With Improved Wasserstein Gradient Penalty and Perceptual Loss," *IEEE Access*, vol. 9, pp. 32795-809, 2021. [CrossRef] [Google Scholar] [Publisher Link]

[16] Dimitrios Korkinof et al., "High-Resolution Mammogram Synthesis Using Progressive Generative Adversarial Networks," *Arxiv Preprint Arxiv:1807.03401*, 2018.[CrossRef] [Google Scholar] [Publisher Link]

[17] Zhongyuan Wang et al., "Ultra-Dense GAN For Satellite Imagery Super-Resolution," *Neurocomputing*, vol. 398, pp. 328-37, 2020. [CrossRef] [Google Scholar] [Publisher Link]

[18] Menglei Zhang, and Qiang Ling, "Supervised Pixel-Wise GAN for Face Super-Resolution," *IEEE Transactions on Multimedia*, 2020 vol. 23, 1938-50, 2020. [CrossRef] [Google Scholar] [Publisher Link]

[19] Agapi Davradou et al., "Diabetic Foot Ulcers Monitoring by Employing Super Resolution and Noise Reduction Deep Learning Techniques," *In proceedings of the 15th International Conference on Pervasive Technologies Related to Assistive Environments* 2022, pp. 83-88, 2022. [CrossRef] [Publisher Link]

[20] M. Langarizadeh et al., "Improvement of Digital Mammogram Images Using Histogram Equalization, Histogram Stretching and Median Filter," *Journal of Medical Engineering & Technology*, vol. 35, no. 2, pp. 103-108. [CrossRef] [Google Scholar] [Publisher Link]

[21] M. C. Shanker, and M. Vadivel, "Hybrid Transfer Learning of Mammogram Images for Screening of Micro-Calcifications," *SSRG International Journal of Electrical and Electronics Engineering*, vol. 9, no. 8, pp. 40-47, 2022. [CrossRef] [Publisher Link]

[22] Fatemeh Pak, Hamidreza Rashidy Kanan, and Afsaneh Alikhassi, "Breast Cancer Detection and Classification in Digital Mammography Based on Non-Subsampled Contourlet Transform (NSCT) and Super Resolution," *Computer Methods and Programs in Biomedicine*, vol. 122, no. 22, pp. 89-107, 2015. [CrossRef] [Google Scholar] [Publisher Link]

[23] Nabin Kharel et al., "Early Diagnosis of Breast Cancer Using Contrast Limited Adaptive Histogram Equalization (CLAHE) and Morphology Methods," *In 2017 8th International Conference on Information and Communication Systems (ICICS)*, pp. 120-124, 2017. [CrossRef] [Google Scholar] [Publisher Link]

[24] Sheeba Jenifer, S. Parasuraman, and Amudha Kadirvelu, "Contrast Enhancement and Brightness Preserving of Digital Mammograms Using Fuzzy Clipped Contrast-Limited Adaptive Histogram Equalization Algorithm," *Applied Soft Computing*, vol. 42, pp. 167-77, 2016. [CrossRef] [Google Scholar] [Publisher Link]

[25] Chaitanya Singla et al., "Deep Learning Enhancement on Mammogram Images for Breast Cancer Detection," *Materials Today: Proceedings*, vol. 49, pp. 3098-104, 2022. [CrossRef] [Google Scholar] [Publisher Link]

[26] Dina A. Ragab, "Breast Cancer Detection Using Deep Convolutional Neural Networks and Support Vector Machines," *PeerJ*, p. E6201, 2019. [CrossRef] [Google Scholar] [Publisher Link]

[27] Mugahed A. Al-antari et al., "A Fully Integrated Computer-Aided Diagnosis System For Digital X-Ray Mammograms Via Deep Learning Detection, Segmentation, and Classification," *International Journal of Medical Informatics*, vol. 117, pp. 44-54, 2018. [CrossRef] [Google Scholar] [Publisher Link]

[28] Felipe André Zeiser et al., "Segmentation of Masses on Mammograms Using Data Augmentation and Deep Learning," *Journal of Digital Imaging*, vol. 33, pp. 858-68, 2020. [CrossRef] [Google Scholar] [Publisher Link]

[29] Ian Goodfellow et al., "Generative Adversarial Networks," *Communication of the ACM*, vol. 63, no. 11, pp. 139-144, 2020. [CrossRef] [Google Scholar] [Publisher Link]

[30] Mingxing Tan, and Quoc Le, "Efficientnet: Rethinking Model Scaling for Convolutional Neural Networks," *International Conference on Machine Learningm*, pp. 6105-6114, 2019. [Google Scholar] [Publisher Link]

[31] Pratheep Kumar P, and V. Mary Amala Bai, "Breast Cancer Detection on Mammographic Images Using Hyper Parameter Tuning & Optimization: A Convolutional Neural Network & Transfer Learning Approach," *International Journal of Engineering Trends and Technology*, vol.70, no. 9, pp. 76-92, 2022. [CrossRef] [Publisher Link]

[32] Ridhi Arora, Prateek Kumar Rai, and Balasubramanian Raman, "Deep Feature–Based Automatic Classification of Mammograms," *Medical and Biological Engineering and Computing*, vol. 58, no. 6, pp. 1199-211. [CrossRef] [Google Scholar] [Publisher Link]

[33] Lenin G. Falconi et al., "Transfer Learning and Fine Tuning in Breast Mammogram Abnormalities Classification on CBIS-DDSM Database," *Advances in Science, Technology and Engineering Systems Journal*, vol. 5, no. 2, pp. 154-65, 2020. [CrossRef] [Google Scholar] [Publisher Link]

[34] J Dafni Rose, "Computer-Aided Diagnosis for Breast Cancer Detection and Classification Using Optimal Region Growing Segmentation with Mobilenet Model," *Concurrent Engineering*, vol. 30, no. 2, pp. 181-9, 2022. [CrossRef] [Google Scholar] [Publisher Link]

[35] Shelda Mohan, and M. Ravishankar, "Modified Contrast Limited Adaptive Histogram Equalization Based on Local Contrast Enhancement For Mammogram Images," *International Conference on Advances In Information Technology and Mobile Communication*, pp. 397-403, 2012. [CrossRef] [Google Scholar] [Publisher Link]